A NEW FOCAL PLANE DETECTOR SYSTEM FOR THE BROAD RANGE SPECTROMETER

CONF-841005--5

DE85 005370

T. P. SJOREEN
Oak Ridge National Laboratory*
Oak Ridge, Tennessee 37831

A focal plane detector system consisting of a vertical drift chamber, parallel plate avalanche counters, and an ionization chamber with segmented anodes has been installed in the Broad Range Spectrometer at the Holifield Facility at Oak Ridge. The system, which has been designed for use with light-heavy ions with energies ranging from 10 to 25 MeV/amu, has a position resolution of ~ 0.1 mm, a scattering angle resolution of ~ 3 mrad, and a mass resolution of ~ 1/60.

1. INTRODUCTION

It is appropriate that this paper presented at the memorial session for J. L. C. Ford, Jr. is about a focal plane detector system. Jim Ford had been involved in research using magnetic spectrometers for nearly two decades and was widely recognized for his contributions to focal plane instrumentation. The focal plane detector system that Jim had been working on was for the Broad Range Spectrometer (BRS) at Oak Ridge. The BRS is a spectrometer which had been used

*Operated by Martin Marietta Energy Systems, Inc. under contract DE-AC05-840R21400 with the U.S. Department of Energy.

extensively during the late 1960's and early 1970's for light-ion spectroscopy. However, with the installation of the new 25 MV tandem, it became apparent that a new focal plane detector system would be needed for heavy-ion spectroscopy.

During 1980 Jim Ford and M. V. Hynes had the idea of using the vertical drift chamber (VDC) as a heavy-ion focal plane detector. Because the VDC was originally designed for nuclear spectroscopy with high energy electrons,[1] it was necessary to build a prototype counter for use with heavy ions. After the counter had been successfully tested, Jim decided to proceed with the installation of a complete focal plane detector system, which could determine the mass, atomic number, charge, and energies of the reaction products. For a discussion of particle identification with magnetic spectrometers see Refs. 2-3. The new detector system which was completed before Jim's death has worked well and Jim's efforts certainly contributed to this success.

2. DETECTOR SYSTEM REQUIREMENTS

There were several requirements which the new detector system had to meet if it was to be useful with the high-energy, high-resolution beams of HHIRF. 1) The position resolution had to better than .25 mm. 2) The detector system had to be able to measure the angle of the particle trajectory. 3) The active length of the detector along the focal plane had to be long enough to measure a 10% range in particle momentum. 4) The system had to be able to function with 10-25 MeV/amu heavy ions. 5) It had to have sufficient mass resolution for studies with projectiles up to mass 40.

The 0.25 mm position resolution was necessary for two reasons. First, the dispersion of the BRS is only about 2 cm/(dp/p)%. Secondly, the Holifield Facility is capable of producing high-resolution beams with dE/E≈1/3500 and energies up to 25 MeV/amu. Thus energy shifts could be as large as several hundred keV/mm. Under such conditions a detector which would contribute more than a few tenths of a mm to the overall linewidth would be useless for high-resolution spectroscopy.

The system had to be able to measure particle trajectory angles so that ray tracing could be performed. This was necessary because the entrance angle aperture of the BRS spans nearly 4° in scattering angle which corresponds to nearly 14° at the focal plane. Thus ray tracing would supply several benefits. 1) Cross sections could be binned in angle. 2) Corrections could be made for magnet aberrations. 3) Time-of-flight (TOF), hence mass resolution, could be improved with path length calculations. 4) Corrections to the energy loss dE/dX could be made to improve both mass and charge resolution.

3. THE DETECTOR SYSTEM

The detector system which was designed to meet the above requirements is shown schematically in Figure 1. The BRS consists of an Elbek dipole[4] later modified by the addition of a vertically focusing quadrupole,[5] that increased the maximum solid angle to 5 msr. The detector spans about 35 cm along the focal plane with a vertical acceptance of 5 cm. This acceptance is compatible with operating the BRS in either the single focusing mode (quad off, vertical image 5 cm) or the double focusing mode (quad on, vertical image about 1 cm). Particles intersect the focal plane at angles

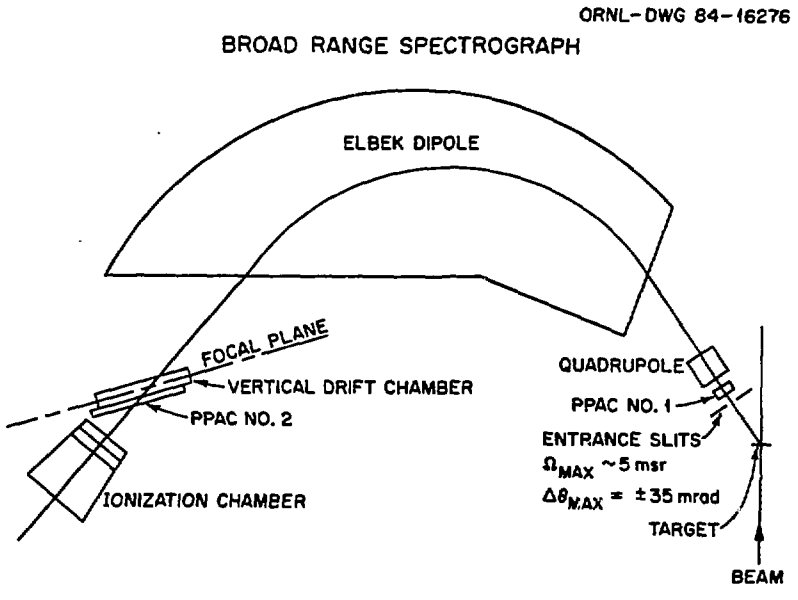

FIGURE 1 Sketch of the BRS and focal plane detectors.

between 30° and 44°.

The VDC is the focal plane counter of this system for measuring the magnetic rigidity B-rho and angle of the reaction products. Behind the VDC is a large parallel plate avalanche counter (PPAC) which provides the start signal for the TOF and the fiducial start for the VDC. Behind these detectors, oriented so that the central ray is normal to the entrance window, is the ionization chamber. This detector measures total energy (E), energy loss (dE/dX), and vertical position. The fourth detector is a small PPAC located just after the entrance aperture and before the quadrupole. It provides the stop signal for TOF.

Details of the operating principle, construction, and performance of the heavy-ion VDC have been described in detail in Refs. 6-7. Here the operating principle and performance are briefly discussed.

A NEW FOCAL PLANE DETECTOR FOR THE BRS

The VDC is a multi-wire proportional counter. As schematically shown in Figure 2, the counter consists of an anode wire plane symmetrically spaced between two high-voltage, aluminized-mylar, cathode planes. The wire plane consists of active sense wires, each separated by two guard wires. The larger diameter, lower-gain guard wires effectively serve to divide the electrostatic volume of the counter into a series of drift cells, each centered around a sense wire. The counter is positioned so that the wire plane is perpendicular to the bending plane of the spectrometer. Thus, particles pass through the first gas-pressure bearing window (not shown), pass through the first high-voltage cathode plane, traverse 4 or 5 adjacent drift cells, and exit through the other cathode plane and pressure bearing window. The free electrons then drift to the anodes where signals are produced. Because the electrostatic field of the drift cells are set so that the drift velocity is uniform, the drift times are proportional to the distance between the trajectory and anode. Thus position and angle can easily be determined if the drift times are measured.

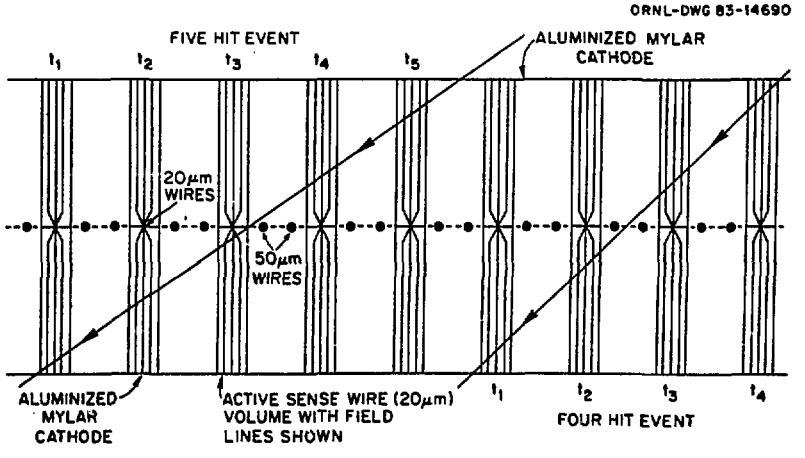

FIGURE 2 Schematic cross sectional view of the vertical drift chamber perpendicular to the anode wires.

The operating characteristics of the VDC were measured with 129-MeV ^{12}C, 176-MeV ^{14}N, and 140-MeV ^{16}O ion beams from the Oak Ridge Isochronous Cyclotron. Measurements were made with isobutane gas at 50, 100, and 200 Torr. The intrinsic cell precision, which is the accuracy to which a trajectory position can be measured in a drift cell, was determined to be about 75 μm. Based on this value we predicted that for trajectories which traverse 4 adjacent drift cells, the position resolution of the VDC should be 0.12 mm FWHM and the angle resolution 6.6 mrad FWHM.

An example of the excellent position resolution of the VDC is shown in Figure 3, which is the distribution of elastic events obtained by bombarding a 100 $\mu g/cm^2$ ^{197}Au target with 176-MeV ^{14}N. The width of this peak is 69 keV FWHM (0.55 mm) for a $dE/E \approx 1/2500$. After considering target and beam contributions to the linewidth, the VDC's contribution to the linewidth is estimated to be ~ 0.1 mm, a value that agrees well with the prediction based upon the 75 μm cell precision estimate.

The angle measuring capability of the VDC is shown in Figure 4, where the distribution of counts obtained by elastically scattering ^{14}N from ^{208}Pb is displayed as a function of the spectrometer entrance angle. To estimate the angular resolution, a mask consisting of four equally spaced wire strips (each 1 mm wide) was positioned between the target and the entrance aperture. The relative positions and widths of the wire mask in the angle spectrum are indicated by the cross hatched areas in Figure 4. The scattering angle subtended by these wires was 3 mrad. From the excellent correlation between the position of the wires and the attenuation of counts in the angular distribution, the scattering angle resolution is estimated to be about 3 mrad.

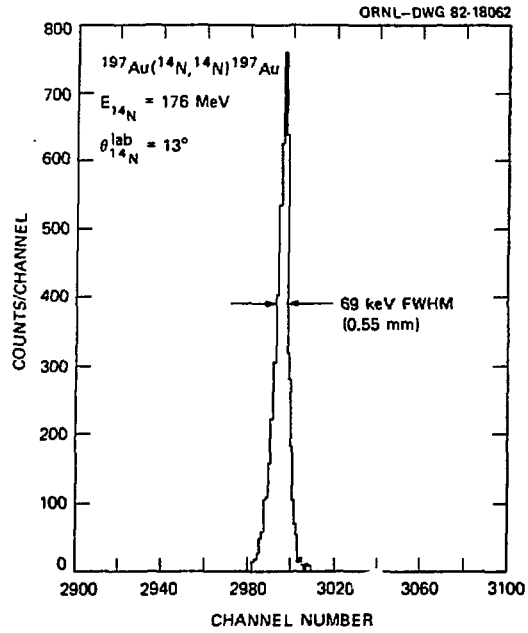

FIGURE 3 Elastic peak obtained with the VDC by scattering 176-MeV ^{14}N from 100 $\mu g/cm^2$ ^{197}Au.

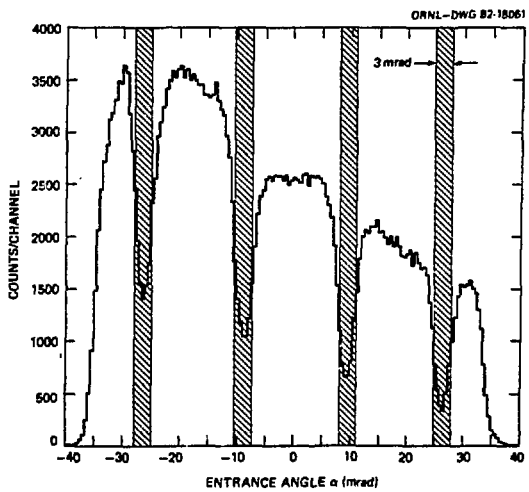

FIGURE 4 Angular distribution of elastically scattered particles as a function of the spectrometer entrance angle. See text for details.

Because there is an angle magnification of about 3.5 between the object (target) and image (focal plane) in the BRS, the 3 mrad value corresponds to about 10.5 mrad at the focal plane. This 10.5 mrad value is about 50% larger than that predicted with the cell precision estimate. This difference is probably due to the finite size of the beam spot.

The ionization chamber for the BRS was designed to be as small as possible, with the conditions that it be able to stop 25 MeV/amu $^{12}C^{6+}$ ions and detect all particles that pass through the VDC and PPAC. Thus the active gas volume of the ion chamber is 40 cm deep, 26 cm wide at the front, 36 cm wide at the back, and 5.4 cm high between the cathode and Frisch grid. The anode-cathode spacing is 6 cm. In addition the anode is segmented into three parts, the first two each 5 cm deep and the last 30 cm, so that energy loss (dE/dX) and total energy (E) can be measured. The chamber has been tested to two atmospheres of gas pressure. Of course, the gas pressure, plate biases, and window thicknesses will depend on the ion species and its energy. For example, with 350 MeV ^{18}O ions, the ion chamber required 900 Torr of isobutane gas, a 50 μm thick Kapton window, and +5600 V and -4000 V biases on the anode and cathode, respectively. Energy loss and total energy resolutions of 2.5% and 1.3%, respectively, have been obtained. A photograph of the ion chamber is shown in Figure 5.

The start detector is a 42 cm long by 5 cm high PPAC which mounts directly on the back of the VDC housing. The detector consists of 3 μm mylar pressure bearing windows and 3 μm aluminized mylar electrodes. The electrode spacing is 3.2 mm. Comparison of the count rates in this detector with those in the ionization chamber indicate a detector efficiency of essentially 100% for 400 MeV ^{16}O ions when

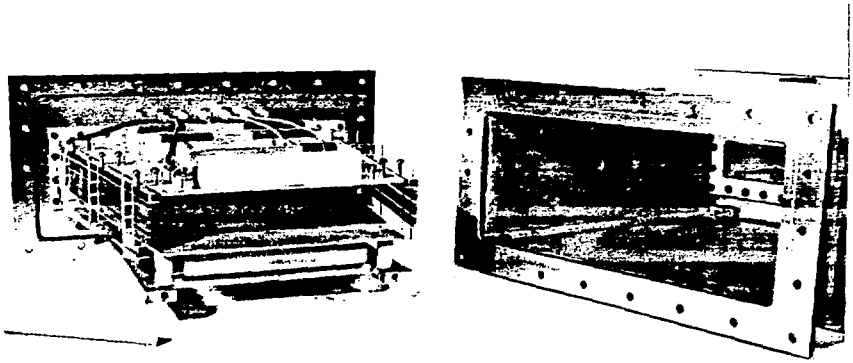

FIGURE 5 Photograph of the ionization chamber.

using 7 Torr of isobutane and a bias of 600 V.

The stop detector, also a PPAC, is 2.54 cm by 2.54 cm. This detector consists of 1.5 μm thick mylar windows and 1.5 μm aluminized mylar electrodes. The electrode spacing is 1.6 mm. It operates with 7 Torr of isobutane at a bias of about 500 V. The total thickness is about 600 $\mu g/cm^2$. This thickness did not affect the resolution of particles detected at the focal plane during tests with 400 MeV ^{16}O.

The timing resolution of the two PPACs is about 600 ps FWHM; this corresponds to a TOF resolution of about 1% for 25 MeV/amu particles.

Figure 6 is a photograph of the three focal plane detectors, i.e. the VDC, the large PPAC, and the ionization chamber. The electronics for the VDC are described in Ref. 7 The electronics for the PPAC and ionization chamber are conventional fast and slow NIM modules. The gas handling system is outlined in Ref. 7 also.

4. SOME RESULTS

After some initial tests with 400-MeV ^{16}O ions, the new detector system was used in two experiments.[8,9] Although

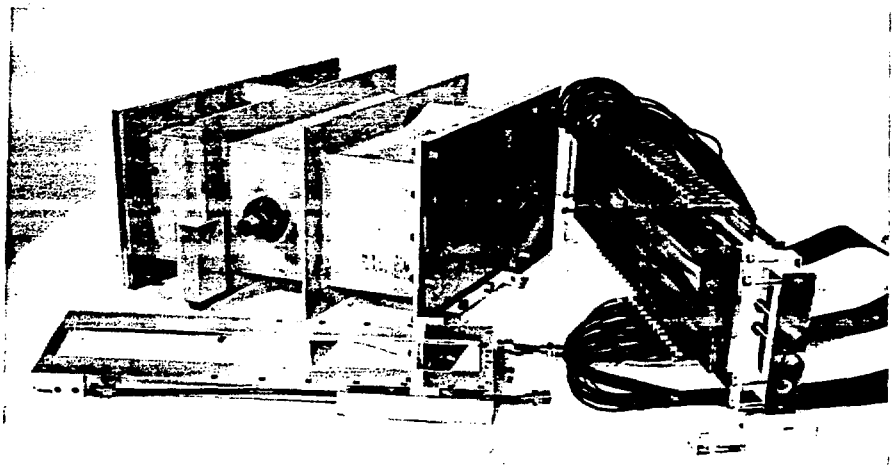

FIGURE 6 Photograph of the VDC, start PPAC, and the ionization chamber.

the analysis of the data is far from complete, the initial indication is that the detector worked quite well, although there were some problems. The next several figures give some indication of the capability of this system.

Figure 7 shows data from the study[8] of spin orbit effects in the $^{28}Si(^{11}B,^{10}B)^{29}Si$ reaction at a 93-MeV bombarding energy. Part (a) shows the correlation between the total energy E and the energy loss in the second anode dE2 for the reaction products in the ion chamber. This is the typical E-dE plot which separates the reaction products into their respective atomic numbers. As shown, the B, Be, and Li products are well separated. Part (b) shows the correlation between focal plane position and E for those boron reaction products which fall inside the contour drawn in part (a). This correlation separates the isotopes for a given element. Part (c) shows those ^{10}B reaction products, that fall inside the contour of part (b), as a function of focal plane position binned into 5 angles. Each angle bin has an acceptance of 0.8 degrees. These spectra were

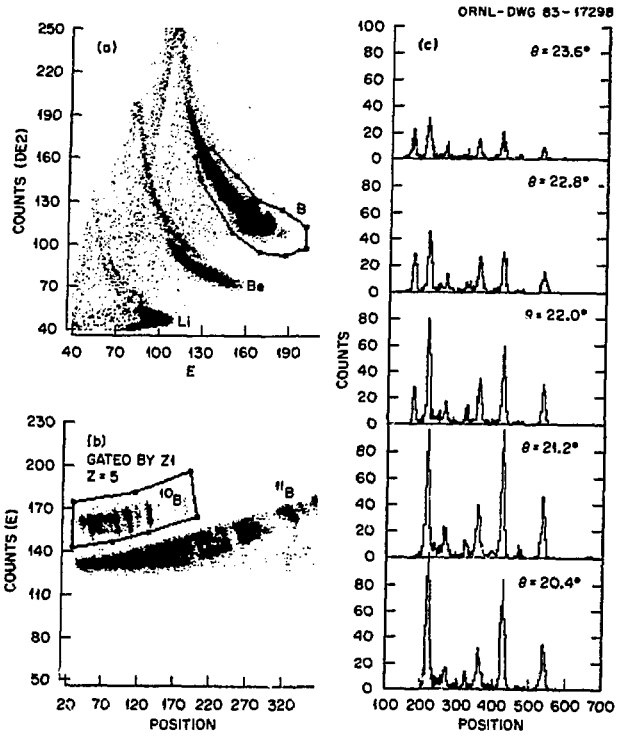

FIGURE 7 Spectra obtained by bombarding ^{28}Si with 93-MeV ^{11}B. See text for a description.

obtained with one angle setting of the spectrometer. The 150-keV FWHM linewidths are due almost entirely to target thickness and beam energy spread.

Figure 8 shows several spectra from the charge exchange study[9] with 350-MeV ^{18}O ions. These spectra, which were taken from a "tune up" run with a Au target, demonstrate the TOF capability. Part (a) is E-dE2 correlation similar to that shown in Fig. 7a. Part (b) is the raw TOF spectrum, with a time resolution of ~ 800 ps. Part (c) shows mass spectra for each of three elements (oxygen, nitrogen, and carbon) using the element identification contours

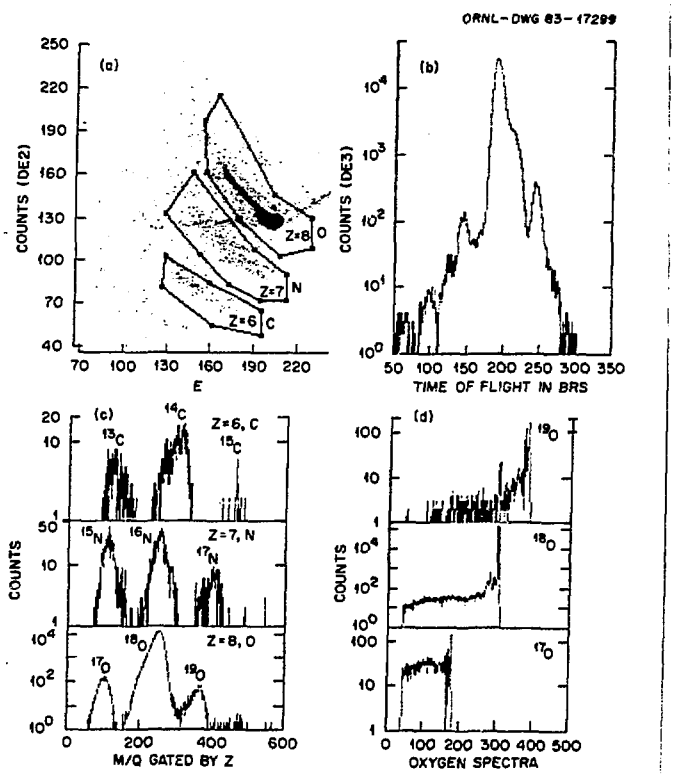

FIGURE 8 Spectra obtained by bombarding ^{197}Au with 350 MeV ^{18}O. These spectra demonstrate time of flight capability. See text for details.

of part (a). The mass distributions were calculated with TOF, E, and angle information. The mass resolution is about 1/60. Part (d) shows focal plane position spectra obtained by gating each of the oxygen isotopes in part (c).

Figures 9 and 10 are more detailed energy spectra obtained during the same experiment with 350-MeV ^{18}O ions on a ^{28}Si target. Figure 9 is a (^{18}O,$^{18}O'$) inelastic spectrum at 6.9 deg (lab), while Figure 10 is an (^{18}O,^{19}F) spectrum at 2.1 deg (lab). The energy resolution of these spectra is about 250-keV FWHM.

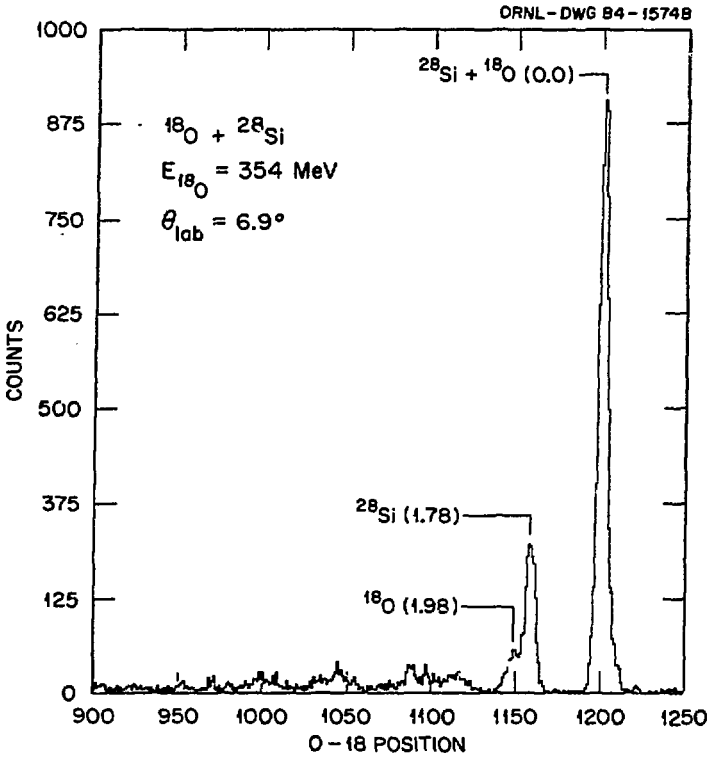

FIGURE 9 Energy spectrum for the $^{28}Si(^{18}O,^{18}O')^{28}Si$ reaction at 350-MeV bombarding energy.

As indicated in the spectra discussed above the detector system has worked well with lighter mass ions $A < 20$ for energies between 10 and 25 MEV/amu. With a mass resolution of 1/60, we anticipate no significant problems with studies up to mass 40.

Recently, the detector system has been used in an experiment with 913 MeV ^{58}Ni on a ^{208}Pb target. It appears that the detector system can be used under these conditions, if care is taken in choosing the operating parameters of the system. In addition, it will be necessary to carefully correct the data to optimize the charge and mass resolution.

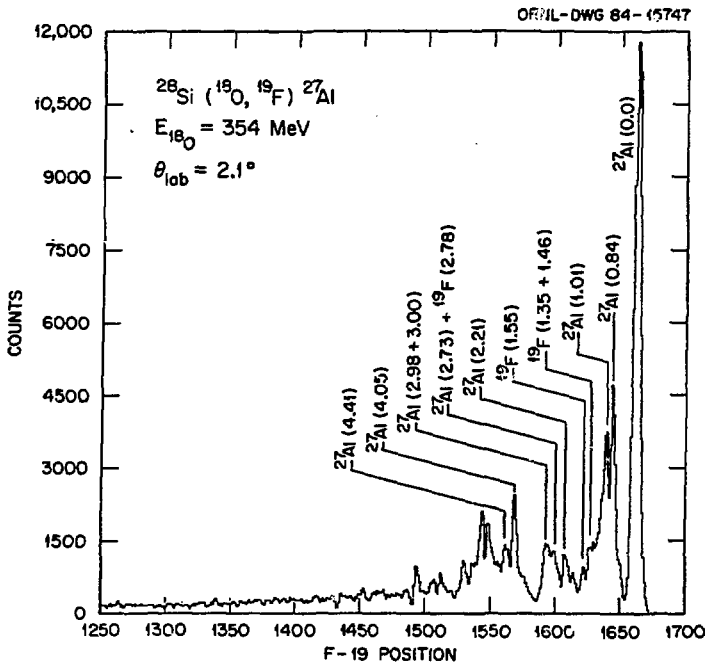

FIGURE 10 Energy spectrum for the ^{28}Si(^{18}O, ^{19}F)^{27}Al reaction at 350-MeV bombarding energy.

Up to now, for projectiles with A ≤ 20, mass identification has been straightforward.

5. CONCLUSIONS

The new detector system for the BRS has met or exceeded our original expectations. The excellent position resolution of 0.1 mm makes it possible to do high resolution spectroscopy with a low dispersion spectrometer such as the BRS. With a scattering angle resolution of ~ 3 mrad (~ 10.5 mrad at focal plane), cross sections can be binned in angle. In addition, corrections for magnet aberrations, TOF pathlengths, and energy loss can be made to increase mass resolution and the usable solid angle of the

BRS. The detector system can easily handle projectile energies between 10 and 25 MeV/amu as well as masses up to A=40 or possibly A=60. With a 10% range in momentum for a given field setting, large ranges of excitation energy can be studied. For example, with 400-MeV ^{16}O on ^{208}Pb, the range of excitation is nearly 100 Mev. In addition multiple charge states and reactions can be detected simultaneously. The versatility of the new system assures much use in the foreseeable future.

ACKNOWLEDGEMENTS

The successful commissioning of the BRS focal plane detector is the result of the efforts of many people. They are R. L. Auble, F. E. Bertrand, J. L. Blankenship, E. E. Gross, D. C. Hensley, and R. O. Sayer of ORNL. D. Schull while on leave from GSI, Darmstadt, and M. V. Hynes provided valuable assistance during the initial tests of the VDC. I would like to thank B. L. Burks for providing Figures 9 and 10.

REFERENCES

1. W. BERTOZZI, M. V. HYNES, C. P. SARGENT, C. CRESWELL, P. C. DUNN, A. HIRSCH, M. LEITCH, B. NORUM, F. N. RAD, and T. SASANUMA, Nucl. Instr. and Meth., 141, 457 (1977).
2. FRED S. GOULDING and BERNARD G. HARVEY, Identification of Nuclear Particles, Ann. Rev. Nucl. Sci., edited by Emilio Segre (Annual Reviews Inc., Palo Alto, CA 94306, 1975), pp. 167-240.
3. J. L. C. FORD, JR., Nucl. Instr. and Meth., 162, 277 (1979).
4. J. BORGGREEN, B. ELBEK, and L. PERCH NIELSON, Nucl. Instr. and Meth., 24, 1 (1963).
5. E. E. GROSS, Nucl. Instr. and Meth., 121, 297 (1974).
6. M. V. HYNES, J. L. C. FORD, JR., T. P. SJOREEN, J. L. BLANKENSHIP and F. E. BERTRAND, Nucl. Instr. and Meth., 224, 89 (1984).

7. T. P. SJOREEN, J. L. C. FORD, JR., J. L. BLANKENSHIP, R. L. AUBLE, F. E. BERTRAND, E. E. GROSS, D. C. HENSLEY, D. SCHULL, and M. V. HYNES, Nucl. Instr. and Meth., 224, 421 (1984).
8. C. F. MAGUIRE, ZHAO KUI, K. TEH, J. L. C. FORD, JR., F. E. BERTRAND, E. E. GROSS, R. O. SAYER, D. SHAPIRA and T. P. SJOREEN, to be published.
9. D. J. HOREN, R. L. AUBLE, F. E. BERTRAND, B. L. BURKS, J. L. BLANKENSHIP, J. L. C. FORD, JR., E. E. GROSS, D. C. HENSLEY, R. O. SAYER, D. SHAPIRA, and T. P. SJOREEN, to be published.

DISCLAIMER